*Revue Roumaine de Chimie,* **2009**, *54*(1), 49–54

# KINETICS OF THE HYDROGEN EVOLUTION REACTION ON 18Cr-10Ni STAINLESS STEEL IN SEAWATER. I. INFLUENCE OF POTENTIAL

Anca COJOCARU,[a] Gabriela Elena BADEA[b], Ioana MAIOR[a], Petru CREȚ[c] and Teodora BADEA[a*]

[a]Department of Applied Physical Chemistry and Electrochemmistry, Politehnica University, Calea Griviței 132, Bucharest-060032, Roumania
[b]Department of Energy Engineering and Management, University of Oradea, Universității 1, Oradea-410087, Roumania
[c]Focus Studio srl, Sovata 40, Oradea-410290 Roumania, contact@mediaoradea.ro

*Received May 21, 2008*

The hydrogen evolution reaction on an 18Cr-10Ni stainless steel electrode in artificial seawater was investigated at temperature of 295K by potentiostatic steady-state voltammetry (PSV) and electrochemical impedance spectroscopy (EIS). The reaction was charge-transfer controlled; it showed a Tafel behaviour and clearly semicircular Nyquist impedance diagrams within the Tafel potential region (-1.2 to -1.62 V). The impedance data was analyzed by a non-linear least square (NLS) fitting program and impedance parameters were evaluated. The high Tafel slope obtained and the chemical rate constant values lead to the assumption that the reaction mechanism is a consecutive combination of the Volmer step followed by the rate-determining Heyrowsky step.

## INTRODUCTION

Hydrogen generation by seawater electrolysis using electricity obtained from regional sources and its subsequent use in fuel cells is one means of reducing environmental pollution resulting from power production based on conventional technologies. The recent increases in cost for fossil fuels and the increased pollution associated with their use give hydrogen the opportunity to provide a practical solution to these problems. From this point of view, water electrolysis, and especially seawater electrolysis, becomes particularly important.[1-4]

In order to produce hydrogen by seawater electrolysis, two key materials are needed: active cathodes for hydrogen evolution during seawater electrolysis, and anodes which effectively evolve oxygen instead of chlorine, even in seawater electrolysis. Platinic metals have the highest activity for the hydrogen evolution reaction,[5] but they cannot be used for large scale hydrogen production. In the last decade, other cathodic materials have shown promise for hydrogen generation, including nickel and a large variety of Ni alloys: Ni,[6-9] Ti-Ni alloys,[10] $Zr_{0.5}$–$Ti_{0.5}$–$V_{0.6}$–$Cr_{0.2}$–$Ni_{1.2}$ alloy,[11] Ni-Mo alloys,[3,12,13] Ni-Fe-C alloys,[4,14] and composite materials such as Ni-P-$TiO_2$-Ti.[15]

Stainless steel is generally considered corrosion-resistant in sea water, and our studies confirmed that 18Cr-10Ni stainless steel shows corrosion resistance in sea water both under open circuit conditions, when it became spontaneously passive,[16] and as a cathode when it is electrochemically protected. Moreover, the principal elements in stainless steel (Fe, Ni and Cr) are excellent catalysts for hydrogen evolution, and are second only to platinum group metals.[5] These are the reasons for use of 18Cr-10Ni stainless steel as the electrode in our study of the HER in seawater.

The aim of this paper is to investigate the kinetics, mechanism of the hydrogen evolution reaction on 18Cr-10Ni stainless steel electrodes in

* Corresponding author: badea_t@yahoo.com

artificial seawater, with the goal of using it as a cathode material during seawater electrolysis. The reaction has been studied at the constant temperature of 295 K, using potentiostatic steady-state voltammetry (PSV) and electrochemical impedance spectroscopy (EIS).

## EXPERIMENTAL

The experimental studies were performed in a classical three-electrode cell with the anodic and cathodic spaces separated by a fritted glass disc. The working electrode (WE), with an exposed surface area of 2 $cm^2$, was made from 18Cr-10Ni stainless steel with the following chemical composition: 18 wt % Cr, 10 wt % Ni, 0.04 wt % C; and 0.33 wt % Si; with the remainder comprised of Fe. The electrode was mechanically polished with 3/0 emery paper, degreased in alkaline solution and rinsed with double distilled water. The counter electrode was a platinum sheet with 4 $cm^2$ surface area. A saturated calomel electrode (SCE) connected with a Luggin capillary served as reference electrode. All potentials quoted in the paper are referred to this electrode.

The solution used was artificial seawater (ASTM D1141 norm[17]) prepared from analytical grade reagents and double distilled water. All measurements were performed at constant temperature of 295 K. Before measurements, the WE was catholically polarized at –1.4 V vs. SCE for 5 minutes to remove some of the surface oxide. After such pre-treatment, no significant hysteresis of the polarisation curve was observed when the measurements were made in the forward (cathodic) or backward (anodic) potential directions.

The cathodic polarisation curve was recorded using in a stepwise technique of 30 mV/60 s in the Tafel potential domain (– 1.2 to –1.62 V vs. SCE). The Tafel potential domain was deduced previously by recording polarisation curves on an extended range of potentials. For PSV measurements, a Radelkis potentiostat was used. The *ac* impedance measurements were carried out with a Bas-Zahner IM6e computer controlled potentiostat in the frequency region of 30 mHz to 50 kHz, at the following constant WE potentials: -0.848, -0.902, -1.200, -1.281, -1.361, and -1.420 V vs. SCE. The fast Fourier transformation (FFT) algorithm was used to obtain the impedance components (real impedance Z', and imaginary impedance Z") at each frequency for the working electrode. Nyquist and Bode diagrams were recorded at constant potentials within the Tafel region of the hydrogen evolution reaction. The impedance parameters were evaluated by nonlinear least square (NLS) fitting.

Because the equilibrium potential of the HER was not established, the 18Cr-10Ni stainless steel presenting spontaneous passivity in artificial seawater, its values were calculated as a function of solution pH. The calculated value of the hydrogen equilibrium potential at the measured pH (6.6) of the solution at 295 K is -0.627 V vs. SCE.

## RESULTS

The Tafel line for the HER on the 18Cr-10Ni stainless steel electrode in artificial seawater is shown in Fig. 1. Insert in Fig.1 is the cathodic polarisation curve on an extended range of potentials. The exchange current density ($i_0$) is determined by extrapolation of the Tafel slope with the calculated hydrogen equilibrium potential. The values of the Tafel slopes ($b$), of the transfer coefficients ($\alpha$) and of the exchange current densities ($i_0$) are respectively: -0.216 $V \cdot decade^{-1}$, 0.27 and $1.67 \times 10^{-6}$ $A \cdot cm^{-2}$.

The experimental electrochemical impedance spectra of the 18Cr-10Ni stainless steel electrode in artificial seawater at four constant potentials taken from the Tafel region of the HER polarisation curve are presented as Nyquist and Bode diagrams in Fig. 2. The diagrams confirm the charge transfer controlled kinetics and show, as expected, a decrease of the charge transfer resistance for the HER with increasing cathodic polarization.

Generally, two models of the equivalent circuit are used for analysis of the influence of certain experimental conditions on complex plane plots obtained for the HER: so called 1CPE[6, 7, 10] and 2CPE[8, 11,] models. By formal statistical analysis it is impossible to distinguish between the two models, as shown by Hitz and Lasia.[8]

The 2CPE model of the equivalent circuit used for the impedance data analysis by nonlinear least squares (NLS) fitting is shown in Fig. 3. This model predicts the formation of two depressed semicircles on the complex plane plots, however only one is usually experimentally observed on many electrodes for the HER.[6-11, 18]

The high-frequency semicircle (CPE-1 –$R_p$), which is independent of the kinetics of the faradaic process[8], contains so called pseudo-capacitance, $C_p$, and pseudo-resistance, $R_p$. This constant phase element is attributed to the mass transfer resistance of the adsorbed intermediate ($H_{ads}$)[6], to the dielectric compound capacitance of the electrode surface[19, 20] or is related to the porosity of the electrode.[8]

The low-frequency semicircle (CPE-2-$R_{ct}$) is related to the kinetics of the faradaic reaction of the HER. The CPE–2 constant phase element corresponds to the double layer capacitance ($C_{dl}$) and $R_{ct}$ is charge transfer resistance.

Fig. 4 shows the Nyquist and Bode form of the theoretical curves (solid lines) and experimental data (points) at -1.281 V vs. SCE, for exemple. The theoretical curves obtained from NLS fitting agree well with the experimental data.

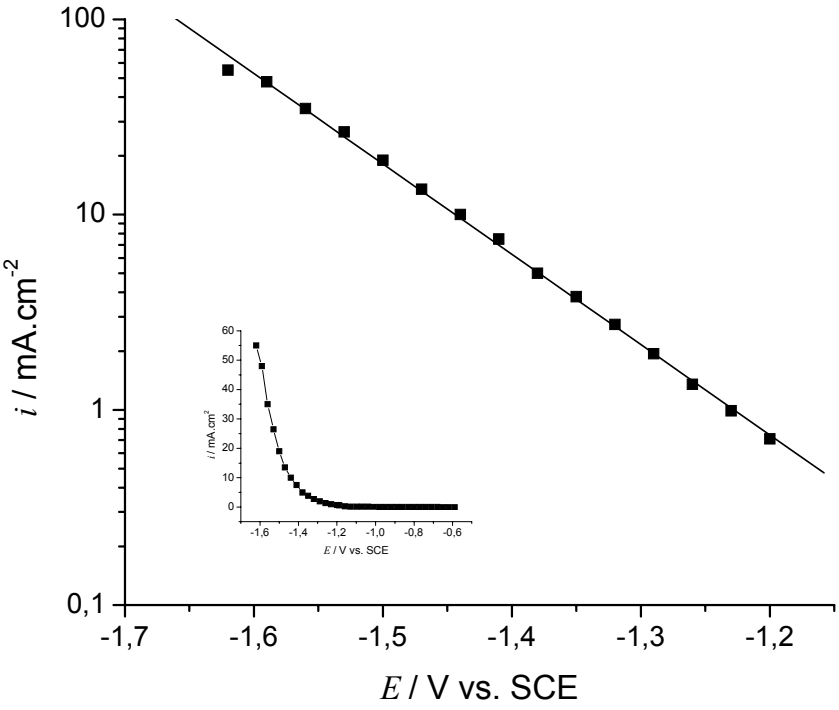


Fig. 1 – Tafel line for the HER on an 18Cr-10Ni stainless steel in artificial seawater, at 295 K. Insert: the polarisation curve on extended potential range.

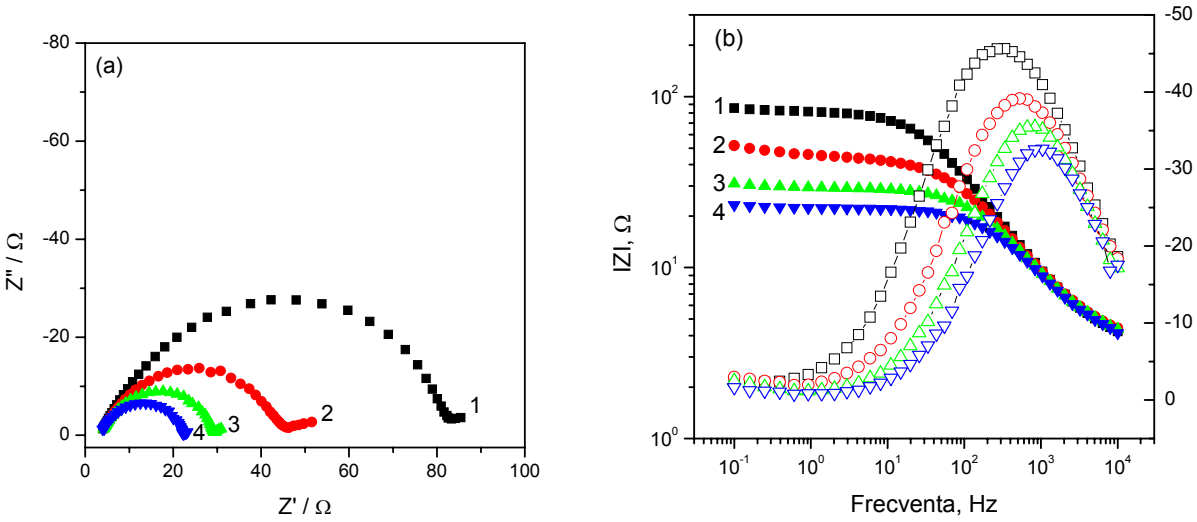


Fig. 2 – Experimental impedance spectra of 18Cr-10Ni stainless steel electrode in artificial seawater as Nyquist plot (a) and Bode plot (b) at various potentials within Tafel region of the HER (V vs. SCE):
1) -1.200; 2) -1.281; 3) – 1.361; 4 -1.420.

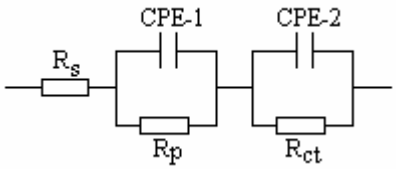


Fig. 3 – Equivalent circuit for NLS fit of the impedance data: $R_s$ – resistance of the solution; $R_p$ – pseudo-resistance $R_{ct}$ – charge transfer resistance; CPE-1 and CPE-2 – constant phase elements corresponding to pseudo-capacitance ($C_p$) and double layer capacitance ($C_{dl}$), respectively.

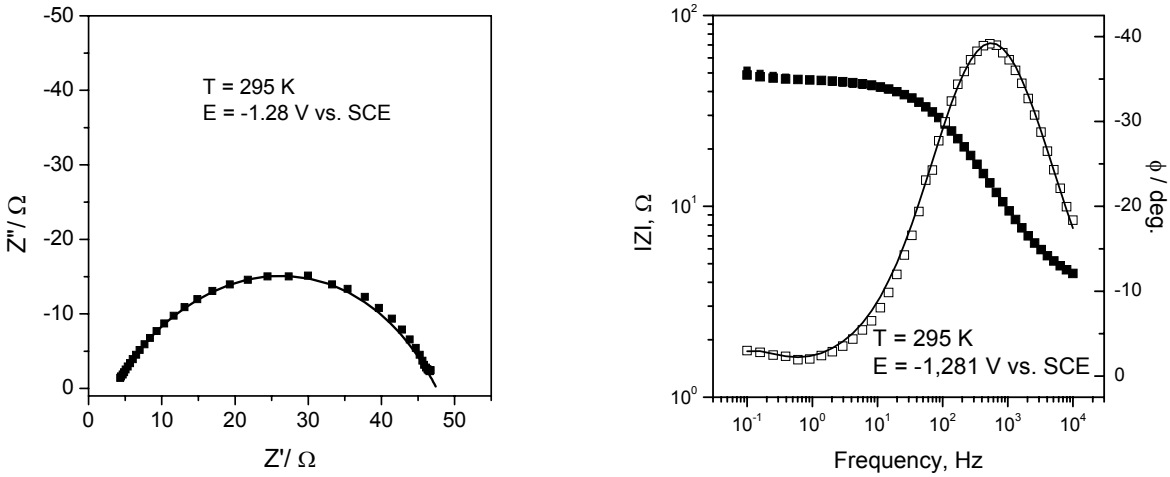


Fig. 4 – The theoretical (as solid curves) and the experimental data (as symbols) impedance spectra in Nyquist (a) and Bode forms (b) obtained from NLS fit results for the HER on an 18Cr-10Ni stainless steel in artificial seawater at 295 K and constant potential (-1.281 V vs. SCE).

The experimentally-obtained impedance parameters are given in Table 1. The charge transfer resistance ($R_{ct}$) decreases significantly with decreasing potential. The double layer capacitance ($C_{dl}$) decreases with increased cathodic overpotential, while the pseudo-capacitance ($C_p$) increases. This behaviour is similar with literature data for the HER on a Ni electrode in 1 M NaOH[7] and in artificial seawater.[9]

*Table 1*

Impedance parameters of the equivalent circuit for the HER at 18Cr-10Ni stainless steel electrode in artificial seawater at 295 K and various potentials

| E<br>V vs. SCE | $R_s$ /<br>Ω | $C_{dl}$ /<br>μF.cm$^{-2}$ | $R_{ct}$ /<br>Ω.cm$^2$ | $C_p$ /<br>mF.cm$^{-2}$ | $R_p$ /<br>Ω.cm$^2$ |
|---|---|---|---|---|---|
| –0.848 | 3.5 | 194 | 4324 | 0.043 | 3.8 |
| –0.902 | 3.6 | 185 | 3426 | 0.043 | 4.2 |
| –1.200 | 3.3 | 170 | 127.9 | 0.126 | 35 |
| –1.281 | 3.6 | 116 | 84.6 | 56 | 12 |
| –1.361 | 3.7 | 89 | 53.6 | 264 | 5 |
| –1.420 | 3.6 | 78 | 37.94 | 650 | 2.4 |

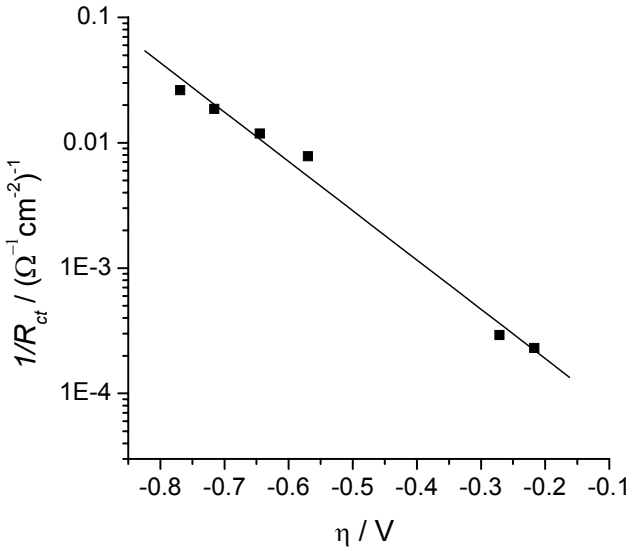


Fig. 5 – Dependence of the charge transfer resistance inverse ($1/R_{ct}$) on overpotential for the HER on 18Cr-10Ni stainless steel electrode in artificial seawater at 295 K.

Since the HER is charge transfer controlled, a plot of log ($1/R_{ct}$) versus polarization ($\eta$) should be linear, as shown in Fig. 5. By extrapolation of the line for $\eta = 0$, the charge transfer resistance at the equilibrium potential of the HER is obtained and exchange current density can be calculated. The value found is $8.8 \times 10^{-7}$ A·cm$^{-2}$, which is reasonably close to the $i_0$ value, obtained from the polarisation measurements.

## DISCUSSION

Generally, in aqueous alkaline and neutral solutions, the HER proceeds through three steps:

$$H_2O + M + e^- = MH_{ads} + OH^- \quad \text{Volmer step} \quad (1)$$

$$MH_{ads} + H_2O + e^- = H_2 + M + OH^- \quad \text{Heyrowsky step} \quad (2)$$

$$2MH_{ads} = H_2 + 2M \quad \text{Tafel step} \quad (3)$$

Consecutive combinations of Volmer (V) and Tafel (T) steps or Volmer and Heyrowsky (H) steps, in which one of them is a rate-determined step, have been proposed for the HER mechanism on various cathodic materials.[3, 6, 8, 10, 11]

The Tafel slope value for the HER on 18Cr-10Ni stainless steel electrode in seawater is higher than the theoretical value ($\partial E / \partial(\log i) = 2RT / F$) if proton discharge is presumed to be the rate-determining step, and $\alpha$ =0.5. High values of the Tafel slopes for the HER were also reported by K. Hashimoto *et al.*[4] for Ni-Mo alloys and by S. Rodrigues *et al.*[11] on $Zr_{0.5}Ti_{0.5}V_{0.6}Cr_{0.2}Ni_{1.2}$ alloy in alkaline solutions.

The consecutive reactions (1) and (2), in which the rate-determining step is the electrochemical desorption of adsorbed hydrogen (*i.e.*, the H step) would be the most likely mechanism for the HER under the present conditions. If the V step is fast and H step is slow, the surface coverage by adsorbed hydrogen will approach unity and the Tafel slope will increase.

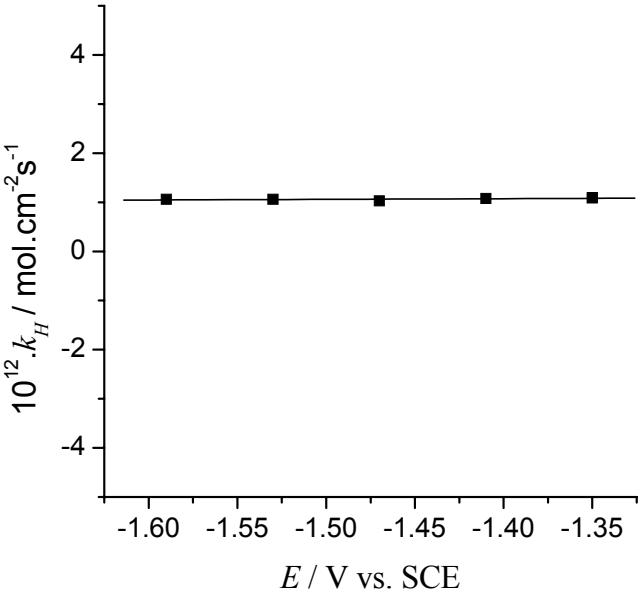


Fig. 6 – Variation with the potential of the chemical rate constant of Heyrowsky step ($k_H$) for the HER on 18Cr-10Ni stainless steel in artificial seawater at 295 K

If it is assumed that the experimentally recorded current densities are determined by the rate of H step ($v_H$) in the potential region E < –1.2 V/SCE, then relation will hold:[6]

$$v_H = k_H \theta_H \exp(-\alpha FE / RT) = i_{exp} / 2F \quad (4)$$

where $k_H$ [mol.cm$^{-2}$.s$^{-1}$] is the chemical rate constant for the rate controlling Heyrowsky step. Taking $\theta_H \approx 1$ and introducing the experimental values for $\alpha = 0.27$ and data from the experimental polarisation curves in Fig. 1 to Eq. (4) for the H step, the chemical rate constants were calculated for various potentials within the Tafel domain. As shown in Fig.6 there is very little variation in the chemical rate constant with the potential, the mean value of $k_H$ having value of $1.06 \times 10^{-12}$ mol.cm$^{-2}$s$^{-1}$. This proves that the H step controls the HER

kinetics on a 18Cr-10Ni stainless steel electrode in artificial seawater.

## CONCLUSIONS

The hydrogen evolution reaction at 18Cr-10Ni stainless steel electrode in artificial seawater is charge transfer controlled: it shows Tafel behaviour and clearly semicircular Nyquist impedance diagrams.

The high Tafel slope obtained and the chemical rate constant values, calculated for the Heyrowsky step, which are practically independent of potential, lead to the conclusion that the reaction mechanism is a consecutive combination of the Volmer step followed by the rate-determining Heyrowsky step.

## REFERENCES


1. L. Popa, E. Guerrini and S. Trasatti, *J. Appl. Electrochem*., **2005**, *35*, 1213-1223.
2. A. A. Temeev, V. P. Belokopitov and S. A. Temeev, *Renwable Energy*, **2006**, *31*, 225-239.
3. K. Hashimoto, H. Habazaki, M. Yamasaki, S. Meguro, T. Sasaki, H. Katargiri, T. Matsui, K. Fujimura, K. Izumiya, N. Kumagai and E. Akiyama, *Mater. Sci. Engng*., **2001**, *A 304-306*, 88-96.
4. K. Hashimoto, M. Yamasaki, S. Meguro, T. Sasaki, H. Katagiri, K. Izumiya, N. Kumagai, H. Habazaki, E. Akiyama and K. Asami, *Corr. Sci*. , **2002**, *44*, 371-386.
5. S. Trasatti, *J. Electroanal. Chem*.,**1972**, *39*, 163-184.
6. N. Krstajić, M. Popović, B. Grgur, M. Vojnović, D. Šepa, *J. Electroanal.Chem*., **2001**, *512*, 16-26.
7. N. Krstajić, M. Popović, B. Grgur, M. Vojnović, D. Šepa, *J. Electroanal Chem*., **2001**, *512*, 27-35.
8. C. Hitz, A. Lasia, *J. Electroanal. Chem.,* **2001**, *500*, 213-222.
9. G. E. Badea, I. Maior, A. Cojocaru and I. Corbu, *Rev.Roum.Chim*., **2007**, *52*, 1123-1130.
10. N.V. Krstajić, B.N. Grgur, N.S. Mladenović, M.V.Vojnović, M.M. Jaksić, *Electrochim. Acta,* **1997**, *42*, 323-330.
11. S. Rodrigues, N. Munichandraiah, A.K. Shukla, *Bull. Mater. Sci*., **2000**, *23*, 383-391.
12. M.R. Gennero de Chialvo, A.C Chialvo*, J. Electroanal. Chem*., **1998**, *448*, 87-93.
13. A. Kawashima, E. Akiyama, H. Habazaki and K. Hashimoto, Mater. Sci. Engng., **1997**, *A 226-228*, 905-913.
14. S. Meguro, T. Sasaki, H. Katargiri, H. Habazaki, A. Kawashima, T. Sakaki and K. Hashimoto, *J. Electrochem. Soc*., **2000**, *147*, 3003-3011.
15. B. Losiewicz, A. Budniok, A. Lasia and E. Lagiewka, *Polish J. Chem*., **2004**, *78*,1457-1476.
16. A. Cojocaru, G. E. Badea, I. Maior and T. Badea, *Cor. Prot. Anticor***.**, **2007**, *2*, 40-46.
17. M. Julia, J. Ferreira and M. Da Cunha Belo, *Portugal. Electrochim. Acta,* **2004**, *22*, 263-278.
18. A. Lasia in B.E. Conway, J.O'M. Bockis, R.E. White (Eds.), "Modern aspects of electrochemistry", No. 32, Kluwwer Academic Publishing, New York, 2002, p. 144-154.
19. M. Drogowska, H. Menard. A. Lasia and L. Brossard, *J. Appl. Elecrochem.*, **1996**, *26*, 1169-1177.
20. C. Gabrielli, M. Keddam, H. Perrot, A. Khalil, R. Rosset and M.Zidoune, *J. Appl. Elecrochem.*, **1996**, *26*, 1125-1132.